

Supporting Information

Allosteric-activation of GDP-bound Ras isoforms by bisphenol derivative plasticisers

Miriam Schöpel¹, Oleksandr Shkura¹, Jana Seidel¹, Klaus Kock¹, Xueyin Zhong¹, Stefanie Löffek², Iris Helfrich², Hagen S. Bachmann³, Jürgen Scherkenbeck⁴, Christian Herrmann¹, and Raphael Stoll^{1,*}

¹ Faculty of Chemistry and Biochemistry, Ruhr University of Bochum, Universitätsstr. 150, D-44780 Bochum, Germany

² Skin Cancer Unit of the Dermatology Department, West German Cancer Center, University Hospital Essen, University Duisburg-Essen and the German Cancer Consortium (DKTK), D-45147 Essen, Germany

³ Institute of Pharmacogenetics, Universitätsklinikum Essen, Hufelandstr. 55, D-45147 Essen, Germany

⁴ Faculty of Mathematics and Natural Sciences, University of Wuppertal, Gaußstr. 20, D-42119 Wuppertal

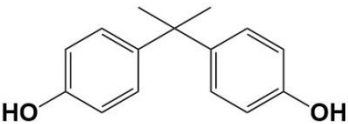
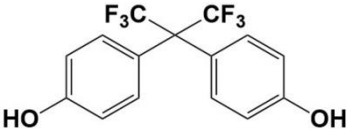
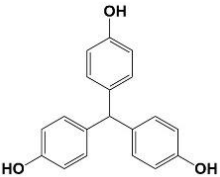
* Correspondence: raphael.stoll@ruhr-uni-bochum.de; Tel.: +49-234-32-25466

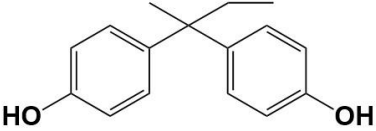
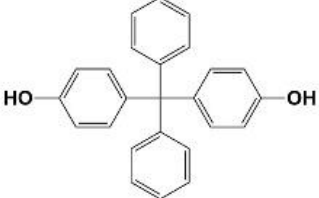
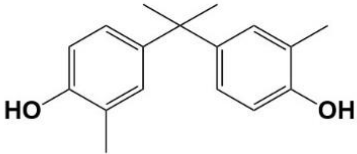
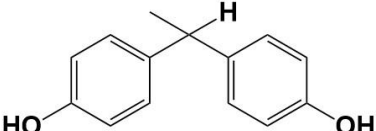
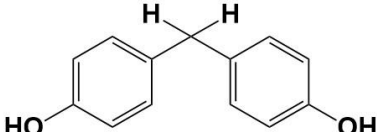
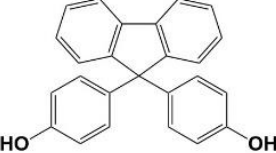
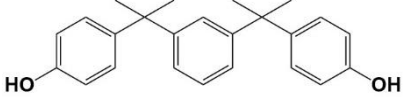
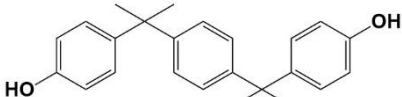
Abbreviations

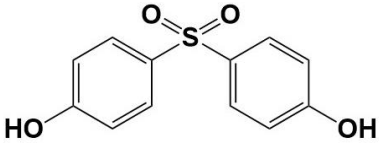
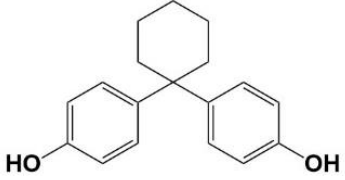
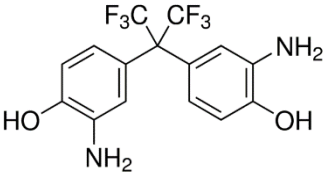
1D, one-dimensional; 2D, two-dimensional; BPs, Bisphenols; BPA, Bisphenol A; BPS, Bisphenol S; EDC, endocrine disrupting chemical; GAP, GTPase activating protein; GDI, guanine nucleotide dissociation inhibition; GDP, guanosine diphosphate; GTP, guanosine triphosphate; GEF, guanine nucleotide exchange factor; HSQC, heteronuclear single quantum coherence; K_D dissociation constant; NMR, nuclear magnetic resonance; RMSD, root mean square deviation; SD, standard deviation; Sos, son of sevenless, BP, bisphenols; BPA, BPAF, BPB, BPE, BPF, BPNH₂.

Table S1

Bisphenols tested in this study, with varying bridging moieties at the central sp³-hybridised carbon atom. AFX was used to characterise the binding of one phenolic ring to K-Ras4B. ND stands for not determined.

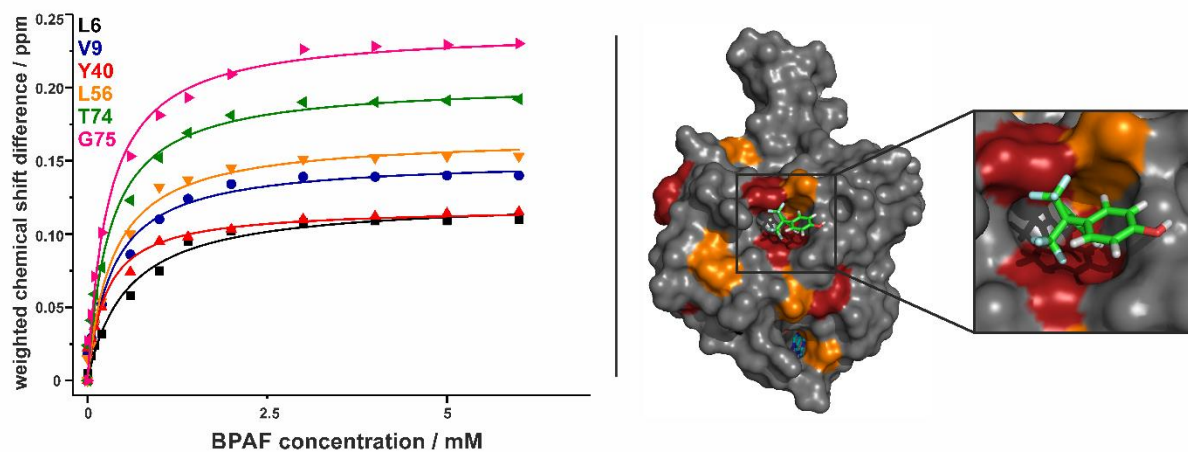
Structural formula	Bis-phenol	CAS	Systematic name (IUPAC)	Comment
	A	80-05-7	2,2-Bis(4-hydroxyphenyl)propane	$K_D=0.6 \pm 0.2$ mM
	AF	1478-61-1	2,2-Bis(4-hydroxyphenyl)hexafluoropropane	$K_D=0.4 \pm 0.1$ mM
	AP	1571-75-1	1,1-Bis(4-hydroxyphenyl)-1-phenyl-ethane	insoluble

	B	77-40-7	2,2-Bis(4-hydroxyphenyl)butane	$K_D=3.6 \pm 0.7$ mM
	BP	1844-01-5	Bis(4-hydroxyphenyl)diphenylmethane	insoluble
	C 2	14868-03-2	Bis(4-hydroxyphenyl)-2,2-dichloroethane	denaturation of protein
	E	2081-08-5	1,1-Bis(4-hydroxyphenyl)ethane	$K_D=7 \pm 0.7$ mM
	F	87139-40-0	Bis(4-hydroxyphenyl)methane	$K_D=14 \pm 2$ mM
	FL	3236-71-3	9,9-Bis(4-hydroxyphenyl)fluorene	insoluble
	M	13595-25-0	1,3-Bis(2-(4-hydroxyphenyl)-2-propyl)benzene	denaturation of protein
	P	2167-51-3	1,4-Bis(2-(4-hydroxyphenyl)-2-propyl)benzene	denaturation of protein

	S	80-09-1	Bis(4-hydroxyphenyl)sulfone	$K_D = 6 \pm 0.7$ mM
	Z	843-55-0	1,1-Bis(4-hydroxyphenyl)-cyclohexane	denaturation of protein
	NH ₂	83558-87-6	1,1-Bis(4-hydroxyphenyl)-cyclohexane	$K_D = 0.4 \pm 0.1$ mM

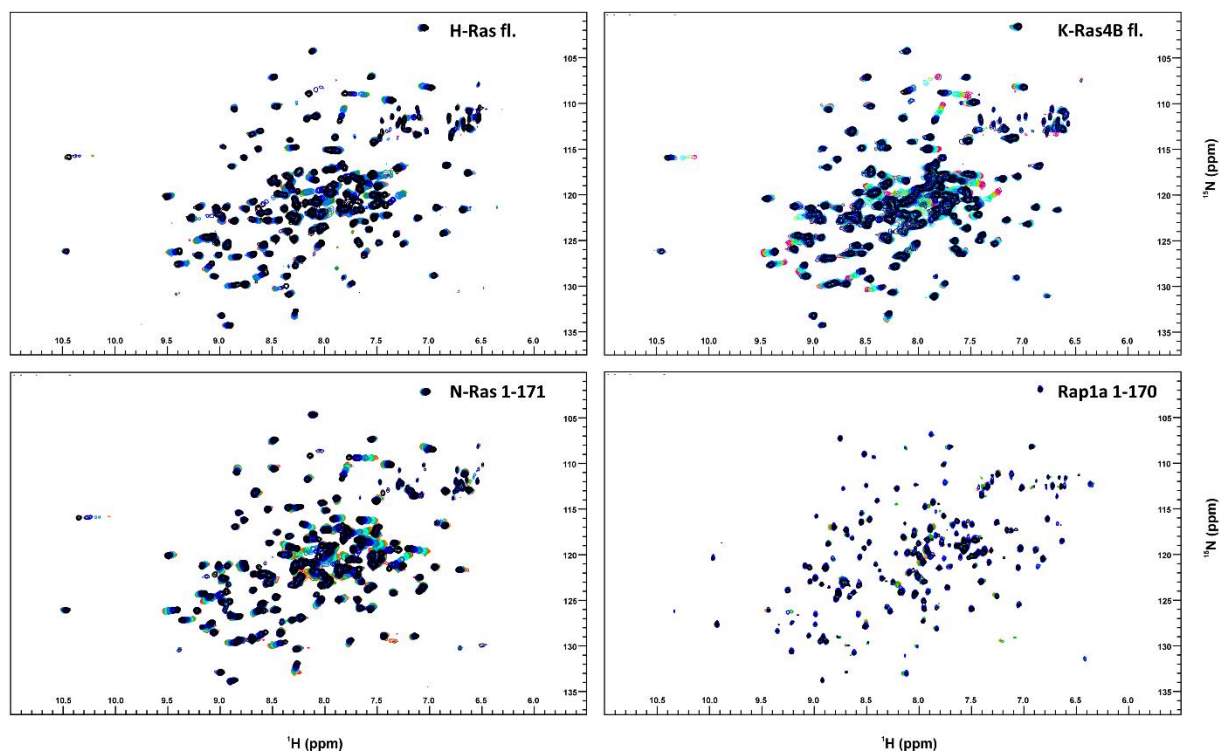
Supporting Figures

Fig. S1



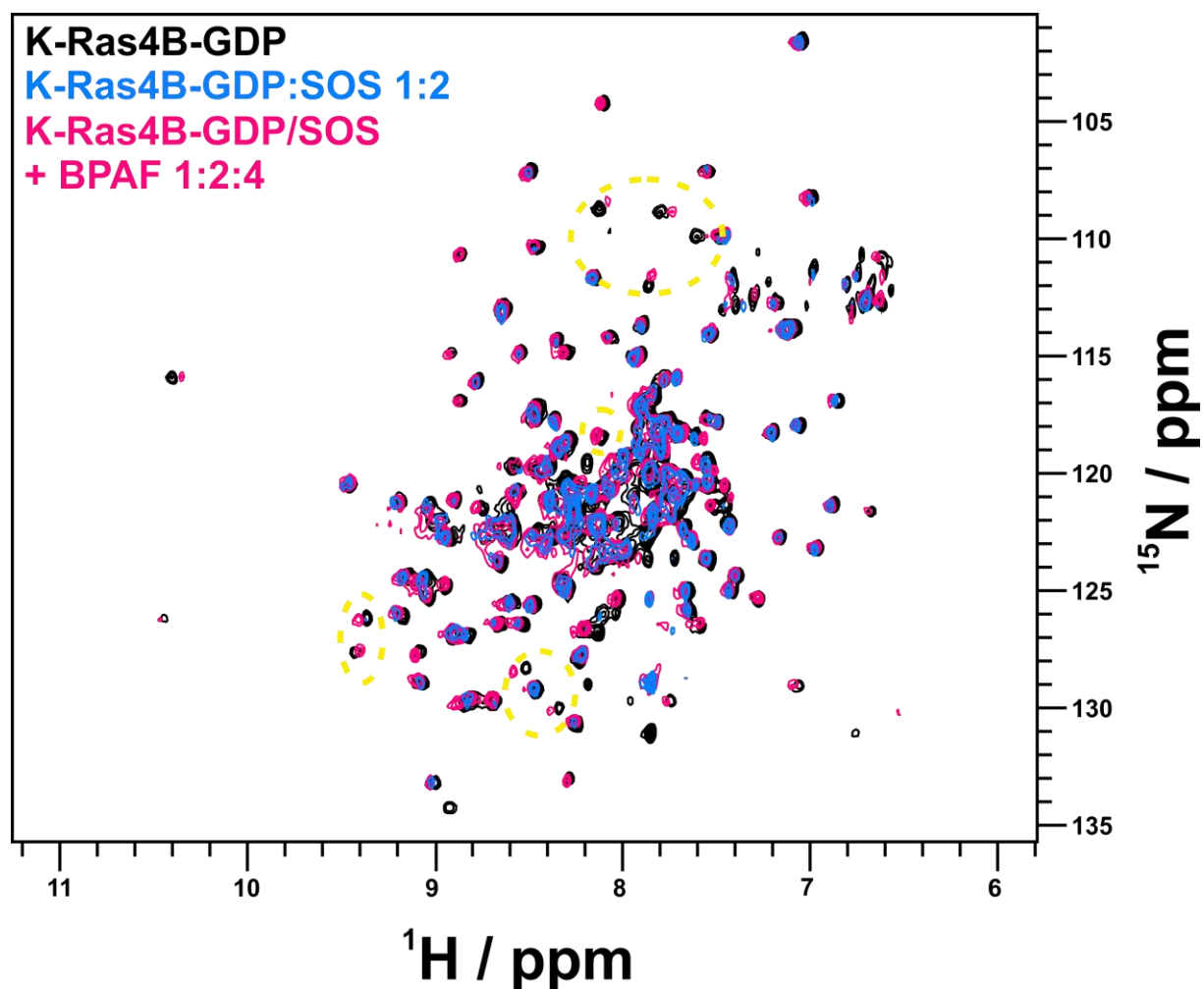
Supporting Figure 1. On the left hand side, the chemical shift differences (in ppm.) are plotted against the ligand concentration (in mM). For the binding pocket, six representative residues (L6, V9, Y40, L56, T74 and G75) were chosen in order to calculate the K_D value that yielded $347 \pm 5 \mu\text{M}$. In the right hand panel, a HADDOCK-based model is shown, in which the amino acids with a weighted chemical shift above once the standard deviation (SD) are annotated in orange and those with a shift with a value twice the SD in red. The BPAF and GDP molecules are represented in green and blue, respectively.

Fig. S2



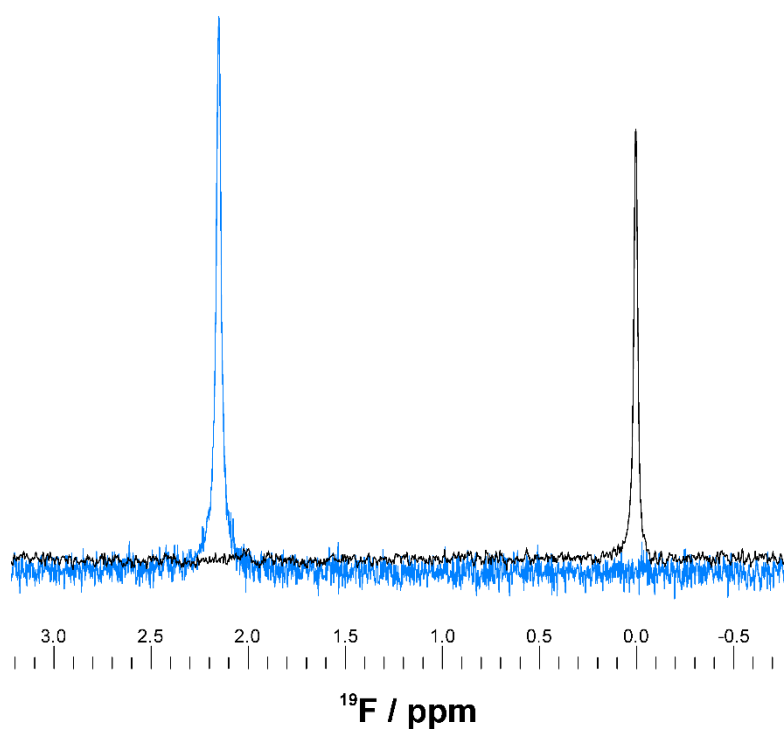
Supporting Figure 2. Overall view of the NMR chemical shift perturbation at 600 MHz and 298 K observed in 2D ^1H - ^{15}N HSQC spectra of H-Ras, K-Ras4B, N-Ras, and Rap-1A bound to GDP upon titration with Bisphenol AF, ranging from the black reference to a ratio of 1:25, shown in magenta. Rap-1A did not show significant binding at all.

Fig. S3



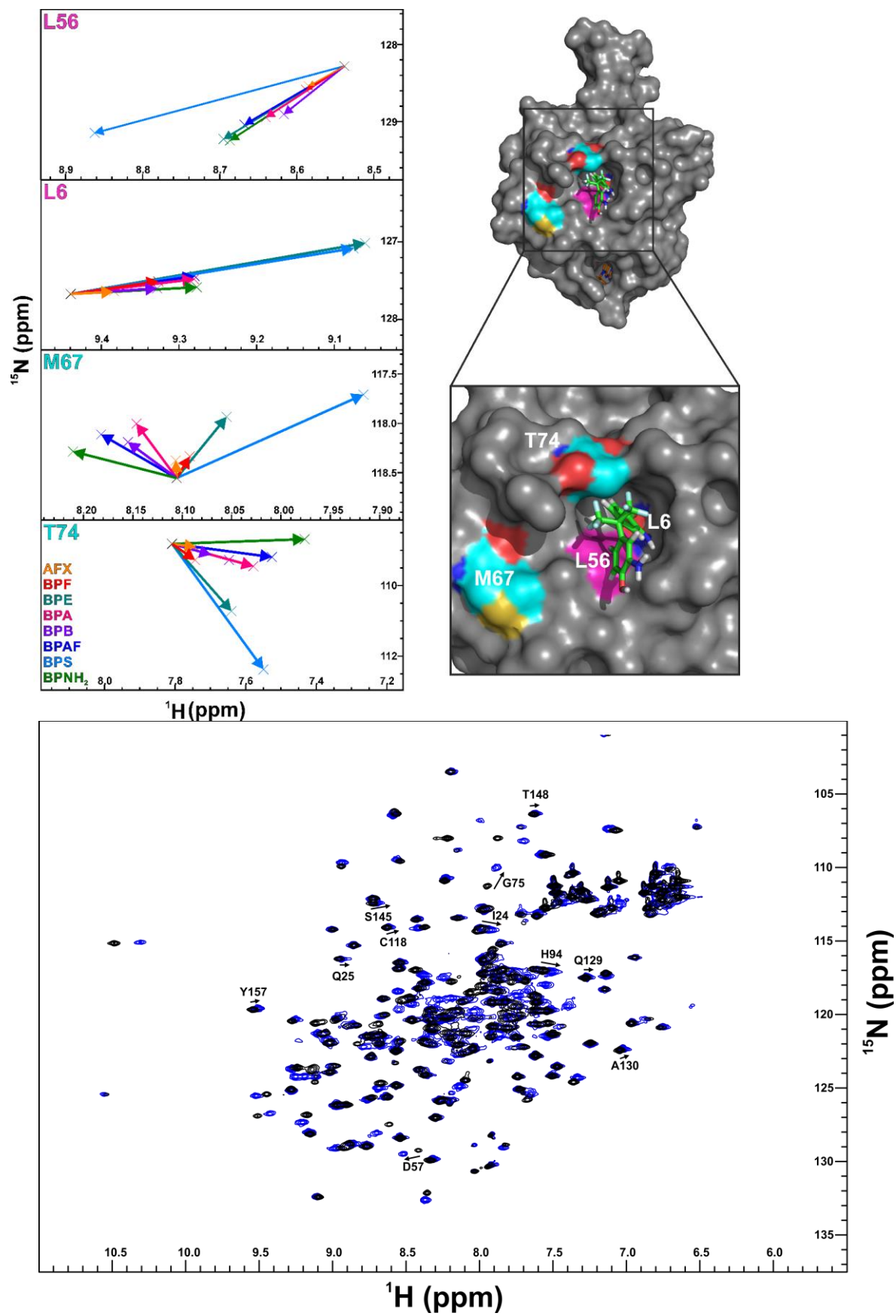
Supporting Figure 3. NMR-based competitive titration of ^{15}N -enriched GDP-bound K-Ras4B with ^{14}N SOS^{cat} and BPAF at 600 MHz and at 298 K. Different 2D ^1H - ^{15}N HSQC spectra of this titration are superimposed. The reference spectrum of the K-Ras4B GDP protein is shown in black. The 2D ^1H - ^{15}N HSQC spectrum of K-Ras4B GDP in the presence of twofold molar excess of the GEF-protein SOS^{cat} is depicted in blue. The 2D ^1H - ^{15}N HSQC spectrum of a sample that contained K-Ras4B GDP, SOS^{cat}, and BPAF in a molar ratio of 1:2:4 is shown in magenta. The recovery of backbone amide proton NMR resonances is indicated by dashed yellow circles. It is important to note that the recovered resonances of residues from the binding pocket exhibit chemical shift perturbations compared to ligand-free 2D ^1H - ^{15}N HSQC spectra of ^{15}N -enriched GDP-bound K-Ras4B that match those observed during the titration of GDP-bound K-Ras4B with BPAF only.

Fig. S4



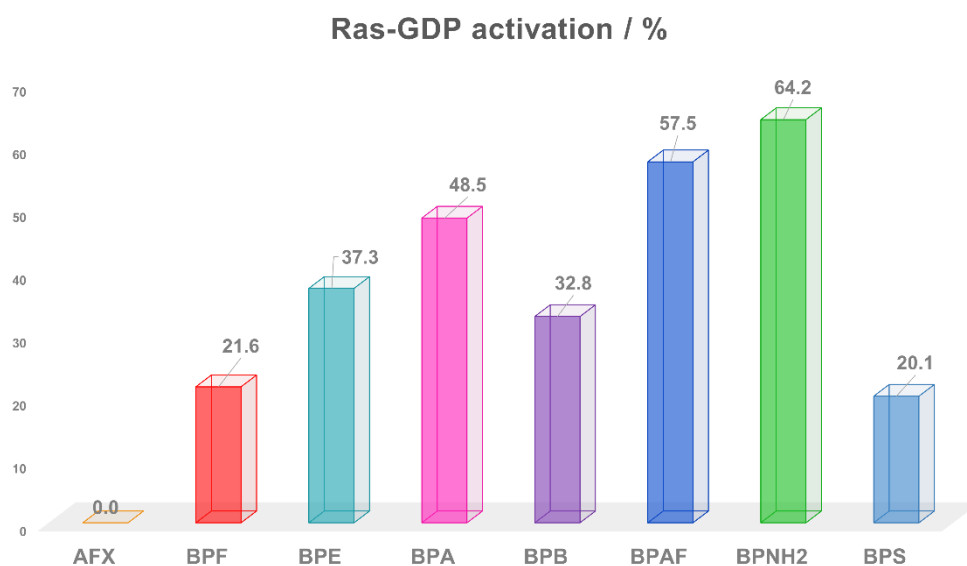
Supporting Figure 4. 1D ^{19}F -Spectra at 235 MHz and at 298 K. In black, the reference BPAF in PBS at pH 7.4 is shown. In blue, the chemical shift corresponding to the protein-bound BPAF (at a molar ratio of 1:1) is presented.

Fig. S5



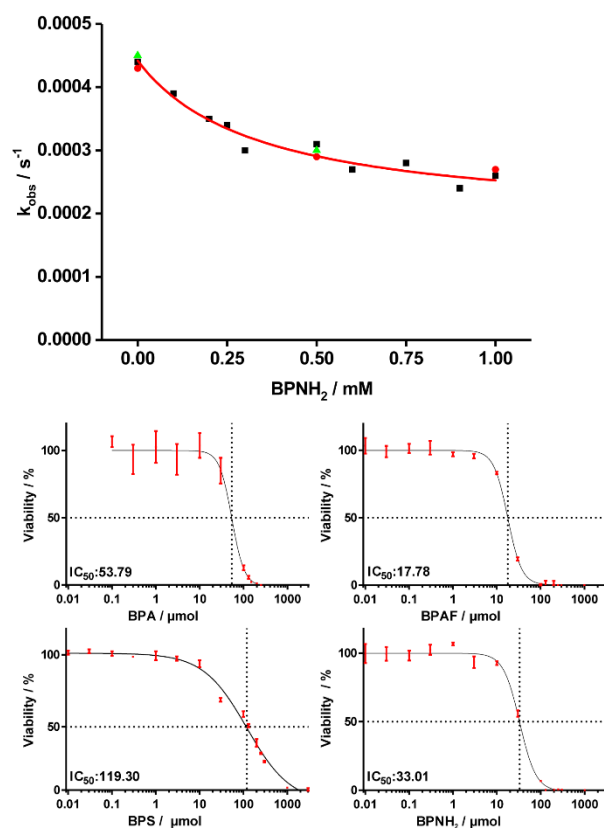
Supporting Figure 5 (refer to previous page). In the upper left hand panel, a vectorial shift analysis of L6, L56 (in pink) as representative residues of the binding pocket is shown based on the addition of BPNH₂ derived from the NMR chemical shift perturbation observed in 2D ¹H-¹⁵N HSQC spectra. The different shifts follow the same pattern, besides of L56 in BPS. In cyan, two representative amino acids from the rim of the binding pocket are shown and the vectorial shift patterns of M67 and T74 are characterised by a high dispersion in the ¹H as well as in the ¹⁵N dimension. In the upper right hand panel, L6, L56, M67, and T74 are highlighted in pink and cyan on the protein surface of GDP-bound K-Ras4B complexed to BPNH₂. The lower part of this figure shows an overlay of 2D ¹H-¹⁵N HSQC spectra of K-Ras4B bound to GDP in the absence (black) and presence (blue) of Bisphenol AF recorded at 700 MHz and 298 K. Chemical shift perturbations observed are highlighted by arrows.

Fig. S6



Supporting Figure 6. Column chart of the activation levels of different bisphenols and AFX (Trifluormethylphenol) based on the chemical shift perturbation of Y157, normalised against the shift of the GppNHp-activated Ras (100%). AFX does not lead to an activation of Ras. In contrast, BPS and BPF cause an activation level of around 20 % each, whereas BPE and BPB induce activation levels of 37.3 % and 32.8 %, respectively. Remarkably, BPA generates an activation level of nearly 50 %, only surpassed by BPAF (57.5 %) and BPNH₂ (64.2 %).

Fig. S7



Supporting Figure 7. GDI assay carried out in triplicate (black, red, green; upper panel): The GDI (guanine nucleotide dissociation inhibitor) assay is carried out similar to the SOS^{cat} assay: Instead of mantGDP, the non-hydrolysable GTP analogue mantGppNHp is used but no SOS^{cat} is added here [17][18]. Again, the dissociation of the fluorescent nucleotide from Ras in the presence of various BPNH₂ concentrations is detected by the decrease of fluorescence and the time dependence yields the k_{obs} values. A plot of the k_{obs} values versus BPNH₂ concentration fitted by a binding isotherm yields the K_D value of the BPNH₂ complex (please also refer to Figure 4). This assay reveals a K_D value of 0.34 ± 0.02 mM for BPNH₂. MTT cytotoxicity assay (lower four panels): The IC₅₀ values in HeLa cells exposed for 72 hrs to BPs were determined as follows: 53.79 μM (BPA), 17.78 μM (BPAF), 33.01 μM (BPNH₂), 119.30 μM (BPS).

Acknowledgements

We are grateful to the Deutsche Krebshilfe (109776 and 109777), the DFG (SFB 642, INST 213/757-1 FUGG), and the RUB Research School^{Plus} for generous financial support.